PROCEEDINGS OF SCIENCE

The nature of the Roberge-Weiss transition in $N_f = 2$ QCD with Wilson fermions

Owe Philipsen, Christopher Pinke*
Institut für Theoretische Physik - Johann Wolfgang Goethe-Universität
Max-von-Laue-Str. 1, 60438 Frankfurt am Main
E-mail: philipsen, pinke @th.physik.uni-frankfurt.de

At imaginary values of the chemical potential μ QCD shows an interesting phase structuredue to its Roberge-Weiss (RW) symmetry. This can be used to constrain QCD at real μ, where the sign problem prevents direct simulations from first principles. Most Lattice QCD (LQCD) investigations of this region have been performed with staggered fermions. In particular, it was found that the RW endpoint, where the RW transition changes from first order to a crossover, depends nontrivially on the quark mass: For high and low masses, it is a triple point, changing to a second order point for intermediate masses. These two regions are separated by tricritical points. A confirmation of these findings using Wilson fermions is presented. In addition, good agreement of a heavy quark effective theory of LQCD for the tricritical point in the heavy mass region with the full LQCD simulations was found.

31st International Symposium on Lattice Field Theory LATTICE 2013
July 29 - August 3, 2013
Mainz, Germany

*Speaker.

PoS(LATTICE 2013)209

1. Introduction

The QCD phase diagram at finite temperature T and chemical potential μ is currently under investigation both theoretically and experimentally, in particular the existence of a critical endpoint (CEP) is of interest. At zero μ, QCD shows a rich phase structure as the quark masses are varied. For infinitely heavy and three flavours of massless quarks, there are first order deconfinement and chiral phase transitions, respectively, at critical temperatures T_c. In the vicinity of these limits, there are regions of first order transitions which are separated by $Z(2)$ second order lines from a crossover region, where the physical point is located. The nature of the transition in the $\mathrm{N_f} = 2$ chiral limit, i.e. whether it is a first or second order transition, is not settled yet. A recent overview is given in [2].

At finite (real) chemical potential, however, the fermion determinant becomes complex. This so-called *sign problem* prevents direct Lattice QCD (LQCD) studies in this region. On the contrary, at purely imaginary values of the chemical potential μ_I there is no sign problem and standard simulation techniques can be applied in a straight-forward way. In addition, QCD exhibits interesting features at μ_I, which can be used to constrain the phase diagram at zero and real μ.

2. QCD at imaginary μ

At finite temperature T and zero chemical potential, gauge transformations Ω have to fulfill periodic boundary conditions in the temporal direction. However, for infinitely heavy quarks the canonical partition function of QCD, $Z_{\mathrm{can}}(T)$, is also invariant if Ω picks up a constant phase z,

$$\Omega(\vec{x},\tau) = z\,\Omega(\vec{x},\tau+1/T)\,. \tag{2.1}$$

z is an element of the center of $SU(\mathrm{N_c})$, $\mathbb{Z}(\mathrm{N_c}) = \left\{ z \in SU(\mathrm{N_c}) | z = \exp(\mathrm{i}\frac{2\pi k}{\mathrm{N_c}})\,, k \in \mathbb{N} \right\}$. This is called *center symmetry*. The breaking of the symmetry is indicated by the *Polyakov Loop*:

$$L(\vec{x}) = \mathrm{Tr}\,\mathscr{P} \exp\left(-\mathrm{i}g \int_0^{1/T} \mathrm{d}\tau A_0(\vec{x}) \right)\,. \tag{2.2}$$

As the loop winds around the temporal direction, it picks up a phase from $\mathbb{Z}(\mathrm{N_c})$. A particular center sector can be identified by its phase: $L = |L|\mathrm{e}^{\mathrm{i}\phi}$. If center symmetry is realised, L will cycle through the different $\mathbb{Z}(\mathrm{N_c})$ sectors and the phases average to zero. Thus, its expectation value $\langle L \rangle$ vanishes, too. However, if the symmetry is spontaneously broken, $\langle L \rangle \neq 0$. For infinitely heavy quarks, this is an order parameter for deconfinement.

At finite μ, the grand canonical partition function $Z(T,\mu)$ can be related to the canonical one via the fugacity expansion:

$$Z(T,\mu) = \sum_n \left(\mathrm{e}^{\beta\mu} \right)^n Z_{\mathrm{can}}(T)\,, \tag{2.3}$$

where the quark number n runs from positive to negative integer values. This implies that $Z(T,\mu) = Z(T,-\mu)$. Considering purely imaginary chemical potential, $\mu = \mathrm{i}\theta/\beta = \mathrm{i}\theta T$, one sees that Z has a periodicity of 2π. Center symmetry is broken explicitly by a finite quark mass: ψ picks up a phase factor z. However, this phase can be accounted for by an appropriate shift in μ: The transformations

$$A_\mu \longrightarrow \Omega A_\mu \Omega^\dagger - \frac{\mathrm{i}}{g}\left(\partial_\mu \Omega\right)\Omega^\dagger, \quad \psi \longrightarrow \Omega\,\psi, \quad \theta \longrightarrow \theta + \frac{2\pi k}{\mathrm{N_c}}\,, k \in \mathbb{N}\,, \tag{2.4}$$

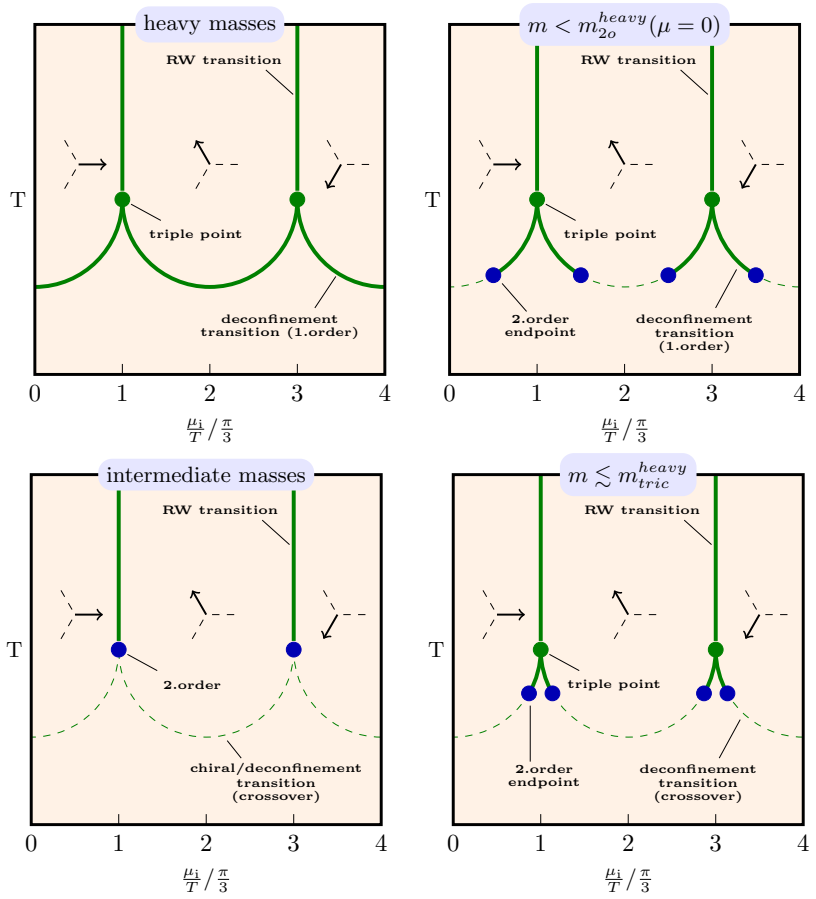

Figure 1: Schematic phase diagram for QCD at imaginary chemical potential (after [9]). The solid vertical lines show the first order RW-transitions at μ_I^c between the different $\mathbb{Z}(\mathrm{N_c})$ sectors, which are indicated by the phase of the Polyakov Loop. Below T_c, the RW transitions are crossover. Beginning in the top left corner, the quark mass is decreased clockwise, changing the chiral/deconfinement phase transition as indicated.

leave Z invariant and unveil a periodicity of $2\pi/\mathrm{N_c}$:

$$Z(\theta) = Z(\theta + 2\pi k/\mathrm{N_c}), k \in \mathbb{N}. \tag{2.5}$$

This is called *extended center symmetry* or *Roberge-Weiss (RW) symmetry* [1]. An order parameter can be defined by introducing the *modified Polyakov loop* $\hat{L} = L\mathrm{e}^{\mathrm{i}\theta} = |\hat{L}|\mathrm{e}^{\mathrm{i}\varphi}$. Its phase again indicates the $\mathbb{Z}(\mathrm{N_c})$ sector the system is currently in and takes on the values

$$\langle\varphi\rangle = k(2\pi/\mathrm{N_c}), k = 0, 1..., \mathrm{N_c} - 1. \tag{2.6}$$

The general phase structure was worked out in [1] and is shown in Figure 1. At critical values

$$\mu_I^c = \mathrm{i}\,(2k+1)\,\pi T/\mathrm{N_c}\ , k = 0, 1 \ldots \mathrm{N_c} - 1, \tag{2.7}$$

there is a phase transition between adjacent $\mathbb{Z}(\mathrm{N_c})$ sectors. Note that due to the periodicity of the partition function of $2\pi/\mathrm{N_c}$ the values of μ_I^c are physically equivalent. At low temperatures the

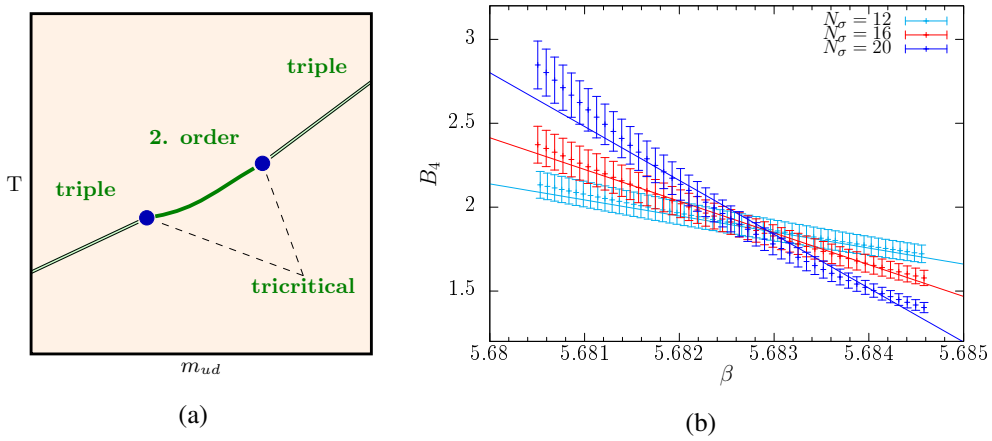

(a) (b)

Figure 2: a) RW endpoint as function of mass (after [9]). b) Reweighted Binder Cumulant of L_{Im} at $\kappa = 0.07$ for various N_σ, including the fits to the finite size scaling form.

transition is a crossover, at high temperatures first order. Consequently, these two regions meet in the *Roberge-Weiss (RW) endpoint*. This point is connected to the deconfinement and chiral transitions at $\mu = 0$. In $\mathrm{N_f} = 2$ and 3 staggered simulations [6, 8] it was found that these transitions extend into the μ_I region and meet the first order RW line in the RW endpoint. Thus, the nature of the endpoint is non-trivial and depends on $\mathrm{N_f}$ and the fermion mass. This is indicated in the figure: For very high masses, the deconfinement transition at $\mu = 0$ is of first order and the RW endpoint is a triple point, as the RW transition and two first order deconfinement transitions meet there. As the mass is lowered, the $\mu = 0$ transition passes through the second order line and becomes a crossover. This carries over to the μ_I region where the second order point approximates the RW endpoint from $\mu = 0$, ending the first order line. The latter is shortened, until it eventually meets the RW point. At this point one has a tricritical point. The same mechanism happens when coming from the chiral limit, increasing the mass, at least for $\mathrm{N_f} = 2, 3$ [6, 8].

Looking only at the nature of the transition in the RW endpoint, one has a triple point for high masses, which for some tricritical mass becomes a second order endpoint. At sufficiently low masses, the endpoint becomes a triple point again, where the first order RW line now meets with two first order chiral transitions lines. This is depicted in Figure 2a. A picture similar to the situation at $\mu = 0$ emerges naturally: For low and high masses there are regions of triple points, which are bounded from a second order region by tricritical lines. For $\mathrm{N_f} = 2 + 1$ the two planes at $\mu = 0$ and $\mu = \mathrm{i}T\pi/\mathrm{N_c}$ must be connected analytically, in particular, the $Z(2)$ lines at $\mu = 0$ become surfaces, meeting the tricritical lines at the RW value. The curvature of the surfaces allows for conclusions about the physical point at real μ. It was found [9] that both the chiral and deconfinement critical surfaces will bend away from the physical point for real μ, which disfavores a CEP. Mapping the (tri)critical surfaces may also allow to clarify the situation in the $\mathrm{N_f} = 2$ chiral limit, see e.g. [10].

3. The Roberge-Weiss transition with Wilson fermions

LQCD studies at μ_I have been carried out predominantly using staggered fermions, in recent years results with Wilson fermions have been presented, too, for example [13, 12]. In the following,

transition type	Crossover	2o 3D Ising	1o triple point	tricritical
$B_4(X)$	3	1.604	1.5	2
ν	-	0.6301(4)	1/3	1/2

Table 1: Values for the Binder cumulant $B_4(X)$ [9] and critical exponent ν for different phase transitions [8].

the nature of the RW endpoint as a function of the fermion mass will be addressed (Figure 2a). This will be done using two flavours of standard Wilson fermions together with the Wilson gauge action and close to the analysis of simulations with three flavours of staggered fermions described in [6]. The confirmation of the structure found in staggered simulations is of high interest as it is used to address the nature of the chiral transition at $\mu = 0$. Additionally, the value of the tricritical mass in the heavy mass region is predicted by an effective theory of LQCD for heavy quarks based on the hopping expansion [11], which states:

$$\kappa_{\text{heavy}}^{\text{tric}} = 0.1048 \pm 0.0008 \,. \tag{3.1}$$

Full LQCD results offer a direct check of the predictive power of the model.

The simulations were carried out utilising CL^{2}QCD [3] on LOEWE-CSC [4] and SANAM [5]. A fixed temporal extent of $N_\tau = 4$ and $\mu_I^c = i\pi T$ have been chosen. Simulations at 24 masses ranging from $\kappa = 0.03 \ldots 0.165$ have been performed. For each κ, at least three, sometimes four or five spatial volumes have been simulated, ranging from $N_\sigma = 8$ to 20. At least ten β-values with $\Delta\beta = 0.001$ around T_c have been simulated for all lattice sizes. In each β run, 35k HMC trajectories of unit length have been produced after 5k trajectories of thermalisation. In some cases this number has been extended to 75k. The acceptance rate in each run was of the order of 75%. Additional β-points have been filled in using Ferrenberg-Swendsen reweighting [16].

The transition at the RW endpoint is a true phase transition only in the thermodynamic limit $V \to \infty$. Thus, to extract it from finite volume LQCD simulations, an extrapolation to the thermodynamic limit must be applied (*finite-size scaling*). This is done by analysing the so-called *Binder cumulant* [15]. For a general observable X, it is defined as

$$B_4(X) = \langle (X - \langle X \rangle)^4 \rangle / \langle (X - \langle X \rangle)^2 \rangle^2 \,. \tag{3.2}$$

B_4 indicates the order of the transition by its value in the thermodynamic limit (see table 1). The finite-size corrections can be described by the ansatz [6]

$$B_4(\beta, N_\sigma) = B_4(\beta, \infty) + a_1(\beta - \beta_c) N_\sigma^{1/\nu} + a_2((\beta - \beta_c) N_\sigma^{1/\nu})^2 + \ldots \,. \tag{3.3}$$

Figure 2b shows the functional behaviour of B_4 as the spatial volume is increased. One sees that B_4 takes on higher values at lower β, going to lower values at higher β, and gets steeper as the volume is increased. This is expected as below and above β_c a crossover and first order region is located, which have a B_4 value of 3 and 1.5 in the thermodynamic limit, respectively. In fact, approaching the thermodynamic limit B_4 should become a step function. The intersection of the three curves is the location of the RW endpoint. The scaling form (3.3) can be fitted to the B_4 data. The obtained value for $B_4(\beta, \infty)$ is found to be somewhat higher then the universal values

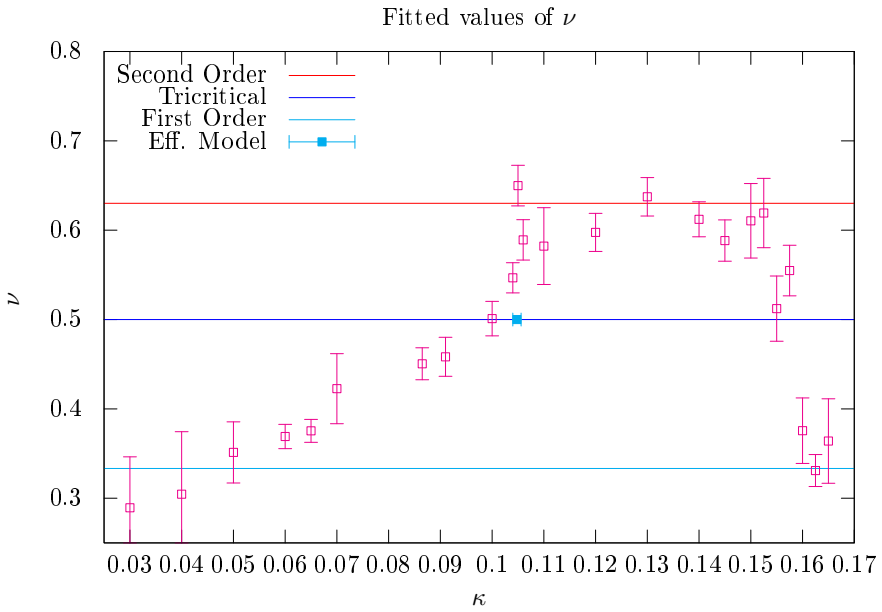

Figure 3: Fitted critical exponent ν as a function of κ. Also shown are values of ν for certain universality classes as well as the prediction for the tricritical mass from the effective theory [11].

because of finite volume corrections, in agreement with [6]. The critical exponent ν, however, can be extracted quite well. This procedure is carried out for all simulated κ and the result of this effort can be seen in Figure 3. The findings with Wilson fermions confirm the staggered results. The extracted value of ν takes on first order values for small κ (high m). The prediction of the effective theory for this point is in good accordance with the observed data. As κ is increased, it passes through the tricritical value until it takes on second order values. As the mass is decreased further, a reverse behaviour can be seen: ν approaches the first order value again, passing through the tricritical value at $\kappa \approx 0.155$.

A similar study has been carried out recently in [13], however, extracting the order of the transition from the scaling of the susceptibility of the imaginary part of L. The authors simulated at various $\kappa \geq 0.155$ and find that these all lie in the first order region. This is partly confirmed by the findings presented here, except that in in [13], no analysis for the tricritical point have been carried out.

4. Summary and Perspectives

QCD at imaginary values of the chemical potential μ_I shows an interesting phase structure, which is currently used to constrain QCD at real μ, where direct simulations from first principles are prevented by the sign problem. Most LQCD investigations of this region have been performed with staggered fermions. In particular, it was found that the RW endpoint depends nontrivially on the quark mass, figure 2a. A confirmation of these findings with Wilson fermions was presented. In addition, good agreement of an heavy quark effective theory of LQCD with the full LQCD simulations was found. In the future, these investigations can be extended to higher N_τ in order to investigate cut-off effects. In addition, a study of the Aoki phase at these parameters would be interesting.

Acknowledgments

O. P, and C. P. are supported by the Helmholtz International Center for FAIR within the LOEWE program of the State of Hesse. C.P. is supported by the GSI Helmholtzzentrum für Schwerionenforschung.

References

[1] A. Roberge and N. Weiss, *Gauge Theories With Imaginary Chemical Potential and the Phases of QCD*, Nucl. Phys. B **275** (1986) 734.

[2] P. Petreczky, *Review of recent highlights in lattice calculations at finite temperature and finite density*, PoS ConfinementX (2012) 028 [arXiv:1301.6188 [hep-lat]].

[3] M. Bach, V. Lindenstruth, O. Philipsen and C. Pinke, *Lattice QCD based on OpenCL*, Comput. Phys. Commun. **184** (2013) 2042 [arXiv:1209.5942 [hep-lat]].

[4] M. Bach, M. Kretz, V. Lindenstruth and D. Rohr, *Optimized HPL for AMD GPU and multi-core CPU usage*, Computer Science - Research and Development (2011), [10.1007/s00450-011-0161-5].

[5] M. Bach, *Twisted Mass Lattice QCD using OpenCL - An Update*, PoS LATTICE **2013** (2013), see also `http://www.top500.org/list/2012/11/`

[6] P. de Forcrand and O. Philipsen, *Constraining the QCD phase diagram by tricritical lines at imaginary chemical potential*, Phys. Rev. Lett. **105** (2010) 152001 [arXiv:1004.3144 [hep-lat]].

[7] P. de Forcrand and O. Philipsen, *The QCD phase diagram for small densities from imaginary chemical potential*, Nucl. Phys. B **642** (2002) 290 [hep-lat/0205016].

[8] C. Bonati, G. Cossu, M. D'Elia and F. Sanfilippo, *The Roberge-Weiss endpoint in $N_f = 2$ QCD*, Phys. Rev. D **83** (2011) 054505 [arXiv:1011.4515 [hep-lat]].

[9] C. Bonati, P. de Forcrand, M. D'Elia, O. Philipsen and F. Sanfilippo, *Constraints on the two-flavor QCD phase diagram from imaginary chemical potential*, PoS LATTICE **2011** (2011) 189 [arXiv:1201.2769 [hep-lat]].

[10] C. Bonati, M. D'Elia, P. de Forcrand, O. Philipsen and F. Sanfillippo, *The chiral phase transition for two-flavour QCD at imaginary and zero chemical potential*, PoS LATTICE **2013** (2013) [arXiv:1311.0473 [hep-lat]].

[11] M. Fromm, J. Langelage, S. Lottini and O. Philipsen, *The QCD deconfinement transition for heavy quarks and all baryon chemical potentials*, JHEP **1201** (2012) 042 [arXiv:1111.4953 [hep-lat]].

[12] A. Alexandru and A. Li, *QCD at imaginary chemical potential with Wilson fermions*, PoS LATTICE **2013** (2013)

[13] L. -K. Wu and X. -F. Meng, *Nature of the Roberge-Weiss transition end points in two-flavor lattice QCD with Wilson quarks*, Phys. Rev. D **87** (2013) 094508 [arXiv:1303.0336 [hep-lat]].

[14] R. D. Pisarski and F. Wilczek, *Remarks on the Chiral Phase Transition in Chromodynamics*, Phys. Rev. D **29** (1984) 338.

[15] K. Binder, *Finite size scaling analysis of Ising model block distribution functions*, Z. Phys. B **43** (1981) 119.

[16] A. M. Ferrenberg and R. H. Swendsen, *Optimized Monte Carlo analysis*, Phys. Rev. Lett. **63** (1989) 1195.